MICROCONTROLLER – BASED DATA PROCESSING FOR NON-LINEAR MEASURING SENSORS

O. Postolache(1), P. Silva Girão(2), J.M. Dias Pereira(3), C. Fosalau(1)

(1) Faculty of Electrical Engineering, Technical University of Iasi, 6600 Iasi, ROMANIA
Phone (40) (32) 130718, Fax (40) (32) 130054, e-mails: poctav@alfa.ist.utl.pt, cfosalau@ee.tuiasi.ro
(2) Instituto de Telecomunicações, DEEC, Instituto Superior Técnico, 1049-001 Lisboa, PORTUGAL
Phone (351) (21) 8417289, Fax (351) (21) 8417672, e-mail: psgirao@alfa.ist.utl.pt
(3) Instituto de Telecomunicações, ESTSetúbal, Instituto Politécnico de Setúbal, 2910 Setúbal, PORTUGAL
Phone (351) (265) 790000, Fax (351) (265) 721869, e-mail: joseper@est.ips.pt

Abstract - *In this paper it is proposed a solution for the numerical linearisation of non-linear parameter dependent sensors. The sensor data-processing architecture combines non-linear analogue to digital conversion with intelligent data processing based on an artificial neural network both implemented using a microcontroller. An application of the processing architecture to gas and vapour concentration measurement is reported.*

Keywords - gas sensor, neural network, non-linear ADC

1. INTRODUCTION

Gas sensors (GSs) are used in several applications, namely in measuring systems for environment quality monitoring.

Tin dioxide semiconductor sensors have a conductance that depends on the reaction at the sensor-to-air-interface at the sensor surface [1]. Because of that characteristic and also because they are simple to use, have a wide spectrum of sensitivity and are quite inexpensive, they are frequently used as gas (or vapour) sensors.

The detection of the presence of a gas in a volume implies only the evaluation whether a certain threshold has been crossed or not. The requirements to implement an electrical gas transducer based on a tin dioxide sensor for that purpose are in theory quite low. However, when the measurement of the concentration of the gas is in stake, the accuracy required is higher. Since tin dioxide sensors have poor selectivity [2][3] and are temperature, humidity and moisture dependent [4], the requirements in what conditioning of sensor output is concerned are then also higher.

Generally speaking, it is possible to increase the performance of a sensor either by hardware conditioning or by software-based conditioning. The implementation of digital signal processing techniques in processor-based devices associated with measuring transducers renders the software solution extremely attractive at present.

The aim of the work now reported is to optimise, based on experimental knowledge of the used sensor, the accuracy of tin dioxide gas sensors through the combination of an intelligent processing of the information related with the temperature and humidity at its surface with an adequate non-linear conversion of the signal delivered by the sensor. The processing makes use of an artificial neural network (ANN) that operating on the normalised temperature and humidity inputs delivers the information necessary for the right establishment of the non-linear converter transfer characteristic.

2. GAS SENSORS-THEORY AND EXPERIMENT

2.1. GSs- Theory

Tin dioxide (SnO_2) semiconductor gas sensors are chosen in the present work considering its wide applicability especially to air quality monitoring. The non-linear characteristics and the disturbance factors of the gas sensor are studied in order to develop an optimal signal processing to increase the performance of gas concentration measurement.

The main feature of the tin dioxide sensors is the dependence of their sensing element conductivity on the detectable gas. Thus, in clean air, the sensor conductivity has a low value increasing with the excitation gas concentration. The conductance in a steady state of the specific sensor (G_{sp}) can be modelled by the following equation [5]:

$$G_{sp} = G_{air} + \alpha_{sp} \cdot C^{\beta_{sp}} \qquad (1)$$

where G_{air} is the sensing element conductance in air, C_{sp} is the concentration of the specific measured gas and α_{sp} and β_{sp} are gas sensor internal parameters that are specific of each tin gas sensor and depend on temperature and humidity. The common values for the $G_{air,}$ α_{sp} and β_{sp} for tin dioxide gas sensors $G_{air} \in$ [5E-6,5E-5] (Ω^{-1}), $\alpha_{sp} \in$ [1E-7, 1E-5] (Ω^{-1}) and $\beta_{sp} \in$ [0.3, 1]. In the particular case of Figaro TGS813 used for CO detection, the proper α_s and β_s values are α_{sp}=9E-7 Ω^{-1} and β_{sp}=0.37.

The main limitation of this type of sensors is selectivity. Even if the sensing element is designed to measure the concentration of only one gas it suffers the effects of interfering gases. An illustrative example: a solvent vapour sensor (TGS822)[6], included in a test chamber (Figaro SR#3) will detect about 10ppm when 100 ppm of hydrogen sulphide are in the chamber and 50 ppm of CO when the chamber is with 100 ppm of ethanol. In both cases the CO concentration in the test chamber is 0 ppm.

The above-mentioned behaviour means that (1) must be changed in order to include terms that take into account the influence of other gases acting on the sensor surface. The specific conductivity G_{sp} in this case is:

$$G_{sp} = G_{air} + \sum_{i=1}^{m} \delta_i \cdot \alpha_{sp} \cdot C_i^{\beta_{sp}} + \alpha_{sp} \cdot C_{sp}^{\beta_{sp}} \qquad (2)$$

where δ_i is an attenuation factor and C_i is the concentration of disturbance gases.

2.2. GS-Experiment

The system used to experimentally study sensors behaviour taking into account humidity and temperature influences (Fig. 1) includes the studied gas sensors (ex. TGS822) with conditioning circuit CC_{GS} (Figaro SR#1), humidity sensor RHS (HS1101)[7] with a conditioning circuit CC_{RH} (HM1500) and the temperature sensor TS (ON-400) with a conditioning circuit CC_T. All of mentioned sensors are inside a test chamber unit (Figaro SR#3). A ventilator and a heater installed in the chamber allow the change of its temperature (T) and relative humidity (RH). The variation of gas or vapour concentration is performed using a dedicated syringe (5cc).

The voltage delivered by CC_{RH} for different values of relative humidity expressed in % is:

$$V_{RH} = V_s \cdot (0.2354 + 0.00474 \cdot RH) \qquad (3)$$

where V_s is the voltage supply (V_s=+5V). For temperature measurement CC_T delivered voltage is:

$$V_T = V_s \cdot \frac{R_{TS}}{R + R_{TS}} \qquad (4)$$

where R_{TS} is the temperature sensor resistance and R is an additional resistance of the CC_T. The $R_{TS}(T)$ dependence is expressed by:

$$R_{TS} = r_0 + r_1 \cdot T + r_2 \cdot T^2 + r_3 \cdot T^3 + r_4 \cdot T^4 \qquad (5)$$

r_0=7355.098 Ω, r_1=-375.8083 Ω °C^{-1}, r_2=10.8047 Ω °C^{-2}, r_3=-0.229 Ω °C^{-3}, r_4=0.003 Ω °C^{-4}

To obtain sensors characteristics required to design an intelligent measuring system based on an ANN and on non-linear conversion, a virtual system that includes a data acquisition board - DAQ (PCI-MIO-16E-4) and a personal computer (PC) is used (Fig. 1).

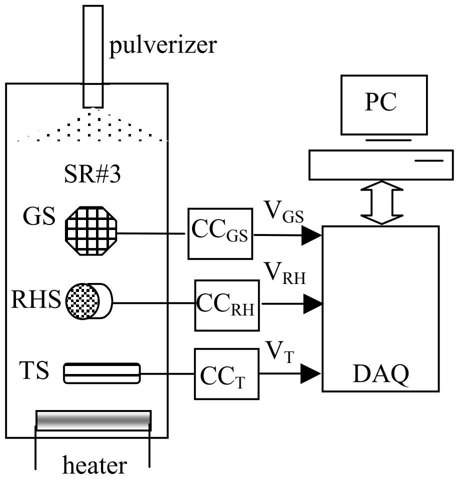

Fig.1 - The virtual system for gas sensors characterisation.

Based on the virtual characterisation system that includes the above-mentioned hardware components (sensors, conditioning circuits, acquisition board and processing unit), the following steps are performed.

1. The system is switched-on, the program for data acquisition and processing is run.
2. Constant values for T and RH are established using the heater-temperature controller and a pulverizer-ventilator based system.
3. A controlled quantity of the measured gas is injected inside on the chamber where the sensors are installed.
4. A delay to permit sensors to reach steady state is allowed.
5. V_{GS}, V_{RH} and V_T are measured to obtain one of $V_{GS}(C_{sp},RH,T)$ characteristic points.

To obtain new points of the same characteristic (RH=RH$_1$, T=T$_1$), new quantities of gas are injected in the test chamber following steps 3-5 of the above-mentioned procedure. Different characteristics are obtained after the test chamber is opened to clean the air and steps 2-5 repeated for new values of RH and T.

Based on the above mentioned procedure, a family of V_{GS}=$V_{GS}(C_{sp})$ characteristics can be obtained. Figure 2 shows such characteristics extracted from data of a TGS822 data sheet when the concentration of ethanol varies between 50-1000 ppm. Humidity and temperature conditions are taken into account and expressed as the parameters that define the family of $V_{GS}(C_{sp})$ characteristics.

Considering the high non-linearity and parameter dependence of the characteristics, a processing scheme is proposed in order to increase the gas measurement system performance with on-line temperature and humidity compensation.

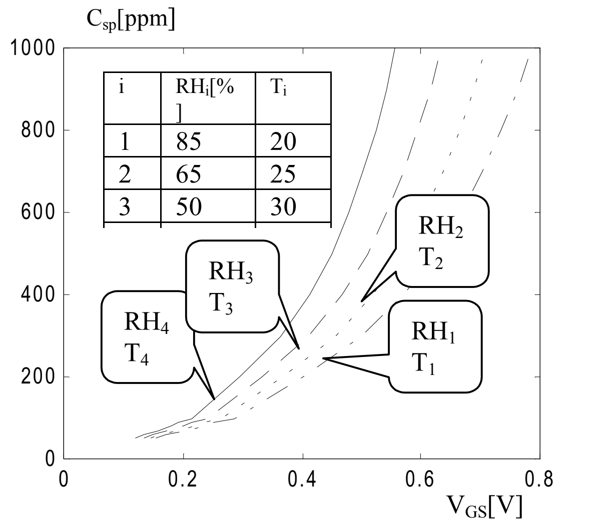

Fig.2 - The humidity and temperature dependence for solvent organic vapours sensor Figaro TGS822. i identifies the curve, e.g. i=1 ⇔ (RH_1 T_1).

3. PROCESSING SCHEME

Based on experimental knowledge of each gas sensor and its dependence with T and RH, an intelligent processing scheme that includes a non-linear converter [8] and an ANN[9][10] is used to perform a 3D modelling associated to C_{sp},(V_{GS}, V_{RH}, V_T). The aim of the modelling is to obtain gas concentration values with an automatic correction of the humidity and temperature disturbance factors. The hardware used to implement the processing scheme is based on a microcontroller in order to assure the portability of the system and a low cost. The block diagram of the proposed scheme is presented in Fig. 3.

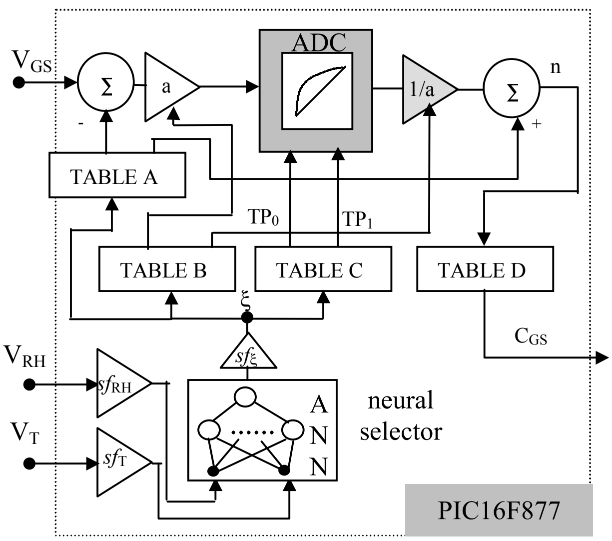

Fig.3 - Gas sensor characteristics -intelligent processing scheme.

The diagram includes the neural selector based on *two-inputs one-output* ANN, a non-linear converter, several normalisation blocks and tables A, B, C and D. Table values are used to normalise V_{GS} values in order to use the non-linear converter capability to obtain directly the code corresponding to gas concentration. Thus, table A includes the offsets of $V_{GS}=V_{GS}(C_{GS}, RH, T)$ curves that are subtracted before non-linear conversion, the correspondent subtraction term in digital form being added at the end of the conversion. Table B is used also for normalisation in order to adapt the values of the $V_{GS}=V_{GS}(C_{GS}, RH, T)$ curve to the non-linear conversion curves, as will be presented in section 3.2. Based on the ANN normalised output (ξ), offset (o_I) and gain (a_I) corrected values are extracted from tables A and B. The same ξ is used to choose the non-linear conversion parameters (Tp_0 Tp_1) from table C. At the end, the digital code n, obtained after conversion and scaling, (division by 'a_i' and addition with 'o_i') is converted into gas concentration using one of table D values.

3.1. The neural selector

The neural selector is used to process the humidity and temperature information delivered by CC_{RH} and CC_T in order to estimate the characteristic of the gas sensor. The purpose of the ANN is to yield the selection parameter ξ for the non-linear ADC in order to compensate the RH and T influences.

Referring to the ANN architecture, the following elements can be mentioned:

- ANN type - multilayer percepton
- number of layers - 3 layers (input layer, hidden layer, output layer),
- number of neurons - 2 input neurons, n_{hidden}=[3;7] hidden neurons, 1 output neuron.
- neuron transfer functions - linear function for output neurons (f_{output}), "tansignoid approximation" function for hidden neurons (f_{hidden}) [9] given by:

$$f_{hidden}(v_k) = \begin{cases} 1 - \dfrac{a}{1+(v_k+b)^3}, & x \ge 0 \\ \dfrac{a}{1-(v_k-b)^3} - 1, & x \le 0 \end{cases} \qquad (6)$$

$$a = 3/2; \quad b = 1/\sqrt[3]{2}$$

where:

$$v_k = w_{k1} \cdot V^N_{RH_{1p}} + w_{k2} \cdot V^N_{T_{2p}} + b_k \qquad (7)$$

In the above relation, w_{k1}, w_{k2} and b_k represent the kth hidden neuron weights and bias. The values of inputs included in the training and test sets are expressed by $V^N_{RH_{1p}}$ and $V^N_{T_{1p}}$ representing the normalised values of the voltages corresponding to RH and T. The normalisation is made using the sf_{RH} and sf_T factors defined as maximum values of V_{RH} and V_T in the operational interval.

The $f_{hidden}(.)$ activation function (6) used to approximate the tanh(x) function is chosen since it is fairly easy to implement in a microcontroller (PIC16F877), requiring only three additions, three multiplications and one division while the tanh(x) implementation requires complex floating point operations [9].

The weights and biases of the ANN are updated by using the Levenberg Marquardt algorithm [11] during the training. The knowledge acquired by the network after learning is stored in its weights and biases in a distributed manner. Signals used for training and testing the network (V_{RH}, V_T) are suitably scaled by appropriate scale factors (sf_{RH}, sf_T) to keep their range within ±1.0. The network output is represented by the index ξ that is also normalised.

The data sets used for ANN training and testing include normalised values V_{RH}^N, V_T^N as input pattern and normalised selection index ξ^N as ANN desired values. The V_{RH}^N, V_T^N pairs correspond to the RH and T values, where T ∈ [10;50] (°C) and RH ∈ [30;85] (%).

In the operational phase, the neural computed ξ is used as search index of tables A, B, and C. Using the n value as index of table D, the C_{GS} concentration is obtained. The modelling of tin film dioxide sensor characteristics shown in Fig.2 is made possible taking into account the capabilities of the proposed non-linear ADC. A brief description of the converter implemented with a microcontroller is presented below.

3.2 The non-linear converter

The basic scheme implemented to perform the non-linear conversion according to the sensor transfer characteristics is presented in Fig.4 [8].

Considering that V_H and V_L are the voltage limits associated to CC_{GS}, the digital code *n* associated to the acquired V_{GS} voltage is:

$$n = \mathrm{int}\left[\frac{V_{GS} - V_L}{(1-k)\cdot V_{GS} + k\cdot V_H - V_L}\cdot 2^B\right] \tag{8}$$

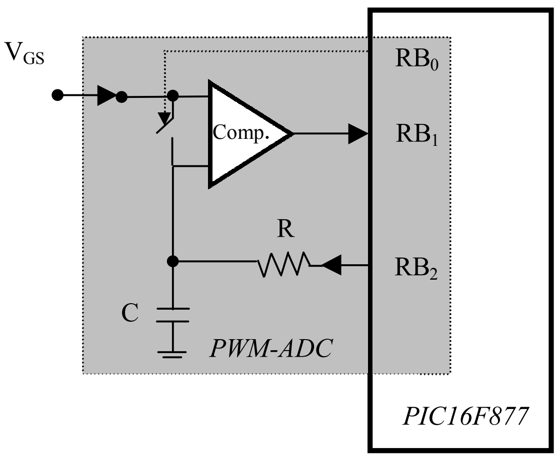

Fig.4 - Microcontroller-based non-linear ADC block diagram.

where *n* is the code conversion value, B the number of bits of the ADC and *k* is the conversion factor defined by:

$$k = 1 - \frac{1-\exp\left(\frac{Tp_1}{RC}\right)}{1-\left(\frac{T_{P0}}{RC}\right)} \qquad Tp_1,\ Tp_0 \ll RC \tag{9}$$

with Tp_1 representing the duration of positive pulse and Tp_0 the duration of negative pulse. For linear conversion k=1 (Tp_0=Tp_1). The values of Tp_0 and Tp_1 impose k and the non-linearity of the ADC. In Fig. 5 several characteristics of the implemented ADC for different k values are presented. The figure also presents the characteristics n=n(V_{GS}) associated to the gas sensor. For different RH and T conditions that conduct to different characteristics (3, 4 or 5), we can apply an optimal gain 'a' in order to adapt the curves to the ADC characteristic expressed by a k factor. In this example the value of offset is considered zero.

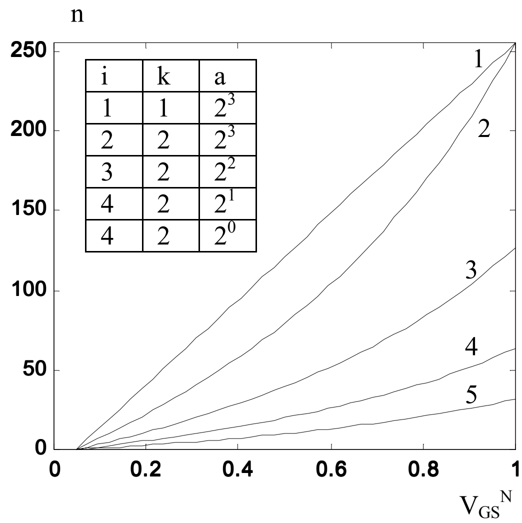

Fig.5 - The ADC non-linear characteristics for different k and amplification values. i is used for curve identification.

Referring to Tp_0 and Tp_1 of table C, Fig. 5 shows two cases: TP_0=TP_1=236μs (k=1) and TP_1=578.2μs, TP_0=236μs (k=2). The values of R and C are R=10^4Ω and C=100nF. V_H is 4.2V and V_L=0.2V.

4. RESULTS

To test the processing method now proposed, catalogue characteristics [6] and several sets of experimental data are considered. The advantage of the experimental data is related to the possibility of covering a wide range of temperature, humidity and concentration of measured gas or vapours. With data extracted from the catalogue, a data acquisition board based simulator is designed in order generate voltages V_{GS}, V_T, V_{RH} corresponding to different values of ethanol concentration included in [50;1000] (ppm) interval, for temperature T∈ [10-30](°C) and the relative humidity RH∈ [30-65](%). The generated voltages are input to the microcontroller and the implemented processing algorithm is tested. The graphic of the absolute error (er_C) calculated as the difference between the concentration imposed to the simulator and the concentration obtained after processing of the voltage acquired by the microcontroller, is presented in Fig. 6. The maximum value of the er_C is less than 40 ppm for an 800 ppm gas concentration representing about 3.5% of full scale, which is a reasonable value for this type of measurement system. It is worth mentioning that for the ranges of temperature and humidity considered, the output voltage of the gas sensor (V_{GS}) would change between some 70% and 120% of standard conditions (T=20ºC and RH=65%).

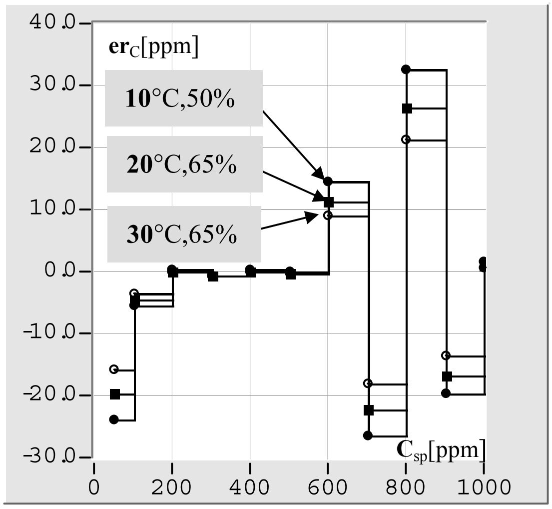

Fig.6 - The evolution of er_C for different values of ethanol vapour concentration taking into account humidity and temperature conditions.

Tests performed using the test chamber, for T=30ºC and RH=50%, confirm the results of simulation. Based on signals acquired from the GS, T and RH sensors for three values of ethanol concentrations (200, 500, and 1000 ppm), the errors obtained are less than 5% of full scale (1000 ppm). Better results can be obtained increasing the non-linear ADC resolution (B>8) and the performance of the ANN selector. In the present case, the implemented neural selector has n_{hidden}=4 neurons. The values of weights and biases are obtained after a 0.93s training cycle, the number of floating point operations required is 70937 and ANN test phase relative approximation error is 0.71%.

5. CONCLUSION

Measuring systems based on non-linear, parameter dependent sensors require adequate treatment of the information delivered by those sensors. The work now presented proposes a mixed hardware-software solution: (a) a virtual neural network working on information of the depending parameters determines the best estimate for the characteristic of the sensor, outputting a parameter that defines the non-linearity of that characteristic; (b) the non-linear parameter is used to define the characteristic of a non-linear analogue-to-digital converter. This processing scheme can be implemented using a microcontroller and its usefulness is being studied in the context of solvent vapours gas sensor. The results obtained are encouraging but final conclusions are only possible after optimisation of the ADC performance and when calibration conditions are practically available.

ACKNOWLEDGMENTS

This work was supported in part by Portuguese Science and Technology Foundation PRAXIS XXI program FCT/BPD/2203/99 and the Project FCT PNAT/1999/EEI/ 15052. This support is gratefully acknowledged. We would also like to thank the Centro de Electrotecnia Teórica e Medidas Eléctricas, IST, Lisboa, for their important technical support.

REFERENCES

[1] F. Sarry, M. Lumbreras, "Gas discrimination in an air-conditioned system", IEEE Trans. Instr. Meas., Vol. 49, No.4, pp. 809-812, Aug. 2000.

[2] J.. Bartolomeo, "Detecting CO in the home", Home automation & building control", pp. 51-55, Oct.1995.

[3] S. Marco, A. Ortega, A. Pardo, J. Samitier, "Gas Identification with Tin Oxide Sensor Array and Self-Organizing Maps: Adaptive Correction of Sensor Drifts", IEEE Trans. Instr. Meas., Vol. 47, No. 1, pp. 316-320, Feb. 1998.

[4] G. Martinelli, M. Garotta, P. Passari, L. Tracchi, "A study of the moisture effects on SnO_2 thick films by sensitivity and permitivity measurements", Sens. Actuat. B [Chemical], Vol. 26-27, pp. 53-55, May 1995.

[5] A. Papadopolus, N. Avaritsiotis, "A model for the gas sensing proprieties of tin oxide thin films with surface catalysts", Sens. Actuat., Vol. 28, pp. 201-210, Sept. 1995.

[6] "TGS822-for detection of organic solvent vapors", -Product information", Figaro USA Inc, 1996.

[7] "Relative Humidity Sensor-HS1100", Humirel Inc, 1999.

[8] J.M. Dias Pereira, O. Postolache, A. Cruz Serra, P. Silva Girão, "A Discrete and Cost Effective ADC Solution Based on a Pulse-Width Modulation Technique", Proc. Confetele 2001, pp. 153-156, Figueira da Foz, Portugal, April 2001.

[9] P. Vehvilainen, H. Ihalainen, '"Estimating the Activation Functions of an MLP-Network", Proc. IMEKO World Congress Wien, Vol. IX, pp. 359-364, Sept. 2000.

[10] J. Patra, A. Kot, G. Panda, “An Intelligent Pressure Sensor Using Neural Netwoks”, IEEE Trans. Instr. Meas., Vol. 49, No. 4, pp. 829-834, Aug. 2000.

[11] M.T. Hagan and M.B. Menhaj, “Training Feedforward Networks with the Marquardt Algorithm”, IEEE Trans. Neural Networks, Vol. 5, No. 6, pp. 989-993, 1994.